

# Unveiling the correlations of tidal deformability with the nuclear symmetry energy parameters

Tuhin Malik,<sup>1</sup> B. K. Agrawal,<sup>2,3</sup> Constança Providência,<sup>4</sup> and J. N. De<sup>2</sup>

<sup>1</sup>*BITS-Pilani, Department of Physics, Hyderabad Campus, Hyderabad - 500078, India*

<sup>2</sup>*Saha Institute of Nuclear physics, Kolkata 700064, India*

<sup>3</sup>*Homi Bhabha National Institute, Anushakti Nagar, Mumbai - 400094, India*

<sup>4</sup>*CFisUC, Department of Physics, University of Coimbra, P-3004 - 516 Coimbra, Portugal*

(Dated: August 11, 2020)

The chi-squared based covariance approach allows one to estimate the correlations among desired observables related to nuclear matter directly from a set of fit data without taking recourse to the distributions of the nuclear matter parameters (NMPs). Such an approach is applied to study the correlations of tidal deformability of neutron star with the slope and the curvature parameters of nuclear symmetry energy governed by an extensive set of fit data on the finite nuclei together with the maximum mass of the neutron star. The knowledge of the distributions of NMPs consistent with the fit data is implicitly inbuilt in the Hessian matrix which is central to this covariance approach. Comparing our results with those obtained with the explicit use of the distributions of NMPs, we show that the appropriate correlations among NMPs as induced by the fit data are instrumental in strengthening the correlations of the tidal deformability with the symmetry energy parameters, without it, the said correlations tend to disappear. The interplay between isoscalar and isovector NMPs is also emphasized.

*Introduction*– The determination of the equation of state (EoS) of nuclear matter over a large density range, much beyond the saturation density  $\rho_0$  is one of the main objectives of both nuclear physics and astrophysics to date [1–3]. The neutron stars (NSs), believed to contain nuclear matter upto few times  $\rho_0$  in their core are the ideal cosmic laboratories to explore the nuclear EoS, complemented with observations from terrestrial experiments. To understand the internal structure of the NS and its properties such as its crust, mass, radius, quadrupole deformation, moment of inertia etc, one needs to connect different branches of physics that include low energy nuclear physics over different density ranges, general theory of relativity and possibly quantum chromodynamics under extreme conditions. Astrophysical observations of NS properties thus open the possibility of lending a complementary vista to constrain the nuclear matter parameters (NMPs) (characterizing the nuclear EoS) in sync with laboratory experiments.

The precise observations of high mass pulsars such as PSR J1614 – 2230 ( $1.908 \pm 0.016 M_\odot$ ) [4], PSR J0348 + 0432 ( $2.01 \pm 0.04 M_\odot$ ) [5] and the recently detected millisecond pulsar J0740 + 6620 ( $2.14^{+0.10}_{-0.09} M_\odot$ ) [6] have already put tight bounds on nuclear matter EoS. Along with precise measurement of the NS masses, future observations such as those planned by NICER (Neutron star Interior Composition Explorer) mission [7, 8], eXTP (enhanced X-ray Timing and Polarimetry) Mission [9], LOFT (Large Observatory For X-ray Timing) satellite [10], and ATHENA (Advanced Telescope for High Energy Astrophysics) [11] may provide besides the mass also the possible range for the radius ( $R_{1.4}$ ) of a canonical NS ( $M = 1.4M_\odot$ ) and other selected NS. The current empirical estimates of  $R_{1.4}$  is  $\simeq 11.9 \pm 1.22$  km [12–16]. Recently NICER came up with one measurement of a

radius  $12.71^{+1.14}_{-1.19}$  km for the NS with mass  $1.34^{+0.15}_{-0.16} M_\odot$  [17, 18]. However, more precise values of masses and radii are required to impose stringent constraints on the EoS. Lately, after the detection of gravitational waves from the GW170817 binary neutron star merger event [19], many authors looked into the rich connection between the quadrupole deformation and the very small nuclear objects more intensely [15, 20–24]. The gravitational wave phase evolution caused by that deformation can be decoded by determining the dimensionless tidal deformability parameter  $\Lambda$  [25–28]. It is a measure of the response to the gravitational pull on the neutron star surface correlating with the pressure gradients inside the NS and strongly depends on the internal structure of the NS or on the EoS. The future precise measurement of  $\Lambda$  and radius of NS can be used as an efficient probe on the investigation of dense nuclear matter EoS.

The correlation systematics has proven to be a useful tool to constrain the EoS, thus the NMPs which are its key ingredients [29–34]. Exploiting the thermodynamic Euler equation and the accepted broad view of nuclear interaction, in a nonrelativistic framework, it has been shown [35] that an EoS for symmetric nuclear matter can be built up and that the thermodynamic state variables of nucleonic matter (energy, pressure, incompressibility etc.) are coupled in a correlated chain. For given values of the energy per particle  $e_0$  and the nucleon effective mass  $m_0^*$ , all at saturation density  $\rho_0$ , the direction of change in the incompressibility coefficient ( $K_0$ ) dictates the direction of change in the skewness parameter ( $Q_0$ ) in such a way so as to keep  $e_0$  invariant. From application of different EoSs intended to give the best fits to the diverse experimental data on a host of finite nuclei, it is found that empirical values of  $e_0$ ,  $m_0^*$  and  $\rho_0$  are obtained with so little scatter that the imprint of the aforesaid correlation is still borne out. For asymmetric nuclear

matter, similar observations are made that the symmetry energy is correlated with higher order density derivatives [36]. Correlations of different nuclear observables are also known to surface out in different contexts; in the ambit of the droplet model, an approximate analytical relation was found between  $L_0$  and the neutron skin thickness [37]  $\Delta r_{np}$  of asymmetric nuclei. This lead to constraining  $L_0$  when  $\Delta r_{np}$  are taken to be known from hadronic probes.

In the recent past, there have been several attempts to constrain the behavior of EoSs from the tidal deformability parameter using a diverse set of mean-field models [15, 23, 38, 39], which satisfy some basic properties of finite nuclei. Similar studies are also carried out to constrain the EoS in a model independent manner [22, 40–44]. In particular, the method of construction of nuclear meta-models [45, 46] based on the Taylor expansion around the saturation density  $\rho_0$  has proved to be useful; the expansion coefficients are identified with the NMPs. Experimental values of the NMPs generate a model independent EoS; this further enables one to study the effects of independent variation of the NMPs on the properties of neutron stars with the allowance to generate models that satisfy on average the constraints set on nuclear matter properties at saturation. A recent result in this context draws particular attention [42]. A regular set of Skyrme or relativistic mean field (RMF) nuclear models [15, 33] fitted to nuclear properties include inherently the correlation among the various NMPs [29, 31]. Whereas these EoSs show a strong correlation of the NS radius or the tidal deformability of the NS with the NMPs, inclusion of a diverse set of EoSs [42] generated from independent variation of NMPs dilutes the correlation casting doubt on the suitability of NS observables on constraining the NMPs. The purpose of this communication is to identify the factors which govern the correlations of tidal deformability with the symmetry energy parameters.

In pursuance of our exploration, we employ a statistical chi-square based covariance approach (CCA) [47] in the Skyrme framework to study the correlations of tidal deformability of neutron stars with the NMPs. This approach enables one to study the correlations between a pair of quantities, consistent with the fit data, with the help of Hessian matrix. In this process the effects of the correlations among various NMPs imposed by finite nuclei are inherently accounted through the Hessian matrix. We also construct large number of EoSs using Multivariate Gaussian Distribution (MVG D) by varying the NMPs independently as well as by including the important correlations among them. Comparison of these results with those obtained within the CCA allows us to identify the most important correlation among NMPs which helps in reconciling the results from different investigations which are at variance otherwise.

*The EoS*– The energy per nucleon,  $e(\rho, \delta)$  for infinite asymmetric nuclear matter in the Skyrme framework depends on the total nucleonic density  $\rho = (\rho_n + \rho_p)$  and

the asymmetry parameter  $\delta = \frac{\rho_n - \rho_p}{\rho}$  as,

$$e(\rho, \delta) = \frac{3}{5} \frac{\hbar^2}{2m} \left( \frac{3\pi^2}{2} \right)^{2/3} \rho^{2/3} F_{5/3} + \frac{1}{8} t_0 [2(x_0 + 2) - (2x_0 + 1) F_2] \rho + \frac{1}{48} t_3 \rho^{\alpha+1} [2(x_3 + 2) - (2x_3 + 1) F_2] + \frac{3}{40} \left( \frac{3\pi^2}{2} \right)^{2/3} \rho^{5/3} \left\{ \left[ \frac{2\theta_s + \theta_{\text{sym}}}{3} \right] F_{5/3} - \frac{1}{2} \left[ \frac{\theta_s + 2\theta_{\text{sym}}}{3} \right] F_{8/3} \right\} \quad (1)$$

$$\text{where } F_m(\delta) = \frac{1}{2} [(1 + \delta)^m + (1 - \delta)^m].$$

The Skyrme parameters  $t_0, t_3, x_0, x_3, \alpha, \theta_s$  and  $\theta_{\text{sym}}$  can be determined from the fit to the plethora of finite nuclear data; expressions for the NMPs such as  $e_0, \rho_0, K_0, Q_0$ , symmetry energy  $J_0$ , its density slope  $L_0$  and the curvature parameter  $K_{\text{sym},0}$  can then be obtained. Conversely, from given values of the NMPs, the seven Skyrme parameters mentioned can be uniquely determined. The parameters  $\theta_s$  and  $\theta_{\text{sym}}$  are measures of the isoscalar and isovector nucleon effective masses, respectively. In this work, we represent the Skyrme EoS as given by Eq. 1 as a point in the seven dimensional space of NMPs,  $e_0, \rho_0, K_0, Q_0, J_0, L_0$ , and  $K_{\text{sym},0}$ . Symbolically, the  $n$ -th EoS in this space is written as

$$\text{EoS}_n^{\text{Skyrme}} = \{e_0, \rho_0, K_0, Q_0, J_0, L_0 \text{ and } K_{\text{sym},0}\}_n \sim N(\boldsymbol{\mu}, \boldsymbol{\Sigma}) \quad (2)$$

where  $N(\boldsymbol{\mu}, \boldsymbol{\Sigma})$  is a MVGD for NMPs with  $\boldsymbol{\mu}$  being the mean value of the nuclear matter parameters  $\boldsymbol{p}$  and  $\boldsymbol{\Sigma}$  the covariance matrix. The diagonal elements of  $\boldsymbol{\Sigma}$  represent the variance or the squared error for the  $p_i$ . The off-diagonal elements of  $\boldsymbol{\Sigma}$  are the covariance between different  $p_i$  and yield the values of the correlation coefficients  $r$  among them. Once, the  $\boldsymbol{\mu}$  and  $\boldsymbol{\Sigma}$  are known a large number of EoSs for the MVGD of NMPs can be obtained.

*Estimation of  $\boldsymbol{\mu}$ ,  $\boldsymbol{\Sigma}$  and  $r$*  – The values of  $\boldsymbol{\mu}$ ,  $\boldsymbol{\Sigma}$  and  $r$  obtained for a single model within the covariance approach are consistent with the fit data. Where as, these quantities calculated for a set of models yields only the model averages. The quantity  $\boldsymbol{\mu}$  within the CCA corresponds to the values of NMPs obtained for the best fit parameters. The covariance of a pair of quantities  $\mathcal{A}$  and  $\mathcal{B}$  can be evaluated within this approach as,

$$\boldsymbol{\Sigma}_{\mathcal{A}\mathcal{B}} = \sum_{\alpha\beta} \left( \frac{\partial \mathcal{A}}{\partial \mathbf{q}_\alpha} \right)_{\mathbf{q}_0} \mathcal{C}_{\alpha\beta}^{-1} \left( \frac{\partial \mathcal{B}}{\partial \mathbf{q}_\beta} \right)_{\mathbf{q}_0} \quad (3)$$

where  $\mathbf{q}_\alpha$  and  $\mathbf{q}_\beta$  are the model parameters and  $\mathbf{q}_0$  represents the set of best fit parameters [47, 48]. The quantities  $\mathcal{A}$  and  $\mathcal{B}$  could be in general either the NMPs, any observables, model parameters or even the mix quantities. The  $\mathcal{C}_{\alpha\beta}^{-1}$  is an element of the inverse of the curvature

or Hessian matrix given by,

$$C_{\alpha\beta} = \frac{1}{2} \left( \frac{\partial^2 \chi^2(\mathbf{q})}{\partial \mathbf{q}_\alpha \partial \mathbf{q}_\beta} \right)_{\mathbf{q}_0} \quad (4)$$

with  $\chi^2(\mathbf{q})$  being the merit function. The covariance  $\Sigma_{\mathcal{AB}}$  is thus consistent with the set of fit data through the matrix  $\mathcal{C}$ . If we consider  $\mathcal{A}, \mathcal{B} = \{e_0, \rho_0, K_0, Q_0, J_0, L_0, K_{\text{sym},0}\}$  which corresponds to a set of seven NMPs as discussed in above, a  $7 \times 7$  covariance matrix can be obtained using Eq. 3. Its diagonal elements  $\Sigma_{\mathcal{AA}}$  are the squared errors and the off-diagonals elements  $\Sigma_{\mathcal{AB}}$  ( $\mathcal{A} \neq \mathcal{B}$ ) are the covariance among them which can be calculated using Eq. 3. The correlations among the pair of quantities  $\mathcal{A}$  and  $\mathcal{B}$  can be quantified using the elements of covariance matrix as,

$$r_{\mathcal{AB}} = \frac{\Sigma_{\mathcal{AB}}}{\sqrt{\Sigma_{\mathcal{AA}} \Sigma_{\mathcal{BB}}}} \quad (5)$$

The absolute value of correlation coefficient  $|r_{\mathcal{AB}}| = 1$  indicates a perfect linear relation between the quantities  $\mathcal{A}$  and  $\mathcal{B}$ . It is usually found that if the correlations among various parameters are strong, then, the errors associated with these individual parameters are also larger. In other words, the correlated errors could be significantly larger than uncorrelated ones [49]. For example stronger correlations among  $K_0 - Q_0$  and  $L_0 - K_{\text{sym},0}$  may result in larger errors on  $K_0, Q_0, L_0$  and  $K_{\text{sym},0}$ . Further, propagation of these errors affects other parameters. The errors on various parameters and correlations among them can not be treated independently and are driven by the fit data in the CCA. Nevertheless, one also often calculates the correlation coefficient  $r_{\mathcal{AB}}$  for a set of models. In this case, the value of  $\Sigma_{\mathcal{AB}}$  is given as [50],

$$\Sigma_{\mathcal{AB}} = \frac{1}{N_m} \sum_i \mathcal{A}_i \mathcal{B}_i - \left( \frac{1}{N_m} \sum_i \mathcal{A}_i \right) \left( \frac{1}{N_m} \sum_j \mathcal{B}_j \right), \quad (6)$$

where the indices  $i, j$  run over the number of models  $N_m$ .

*Results*– The correlation between a pair of quantities within the CCA is calculated using the Hessian matrix which is consistent with the set of fit data. We use this approach to study the correlations of the tidal deformability with the slope and curvature of nuclear symmetry energy and generate the confidence ellipses which are consistent with the selected ground and excited state properties of finite nuclei as well as with the maximum mass of NSs. The ground state properties of finite nuclei considered are the binding energy and charge radii. The excited state properties considered are the isoscalar giant monopole resonance energy and the dipole polarizability. Alternatively, the correlations of the tidal deformability with symmetry energy parameters are studied using a set of EoSs obtained by varying the NMPs independently. In this process, the correlations among the various NMPs as imposed by the fit data are ignored. In the following,

Table I. The mean value  $\mu_{p_i}$  and error  $\sqrt{\Sigma_{p_i p_i}}$  for the nuclear matter parameters  $p_i$  employed for the multivariate Gaussian distribution. All the quantities are in the units of MeV except for  $\rho_0$  which is in unit of  $\text{fm}^{-3}$ . We sample our EoSs for three different cases; see text for details. The NMPs corresponding to SkA267 model are also listed.

$p_i$	MVG D		SkA267	
	$\mu_{p_i}$	$\sqrt{\Sigma_{p_i p_i}}$	$\mu_{p_i}$	$\sqrt{\Sigma_{p_i p_i}}$
$e_0$	-16.0	0.25	-16.04	0.2
$\rho_0$	0.16	0.005	0.161	0.002
$K_0$	230.0	20	230.2	6.1
$Q_0$	-300	100	-366.8	12.0
$J_0$	32.0	3	31.4	3.1
$L_0$	60.0	20	41.1	18.2
$K_{\text{sym},0}$	-100.0	100	-124.0	70.2

we will present our results obtained for independent and correlated MVGD of NMPs and compare them with the ones obtained using the CCA.

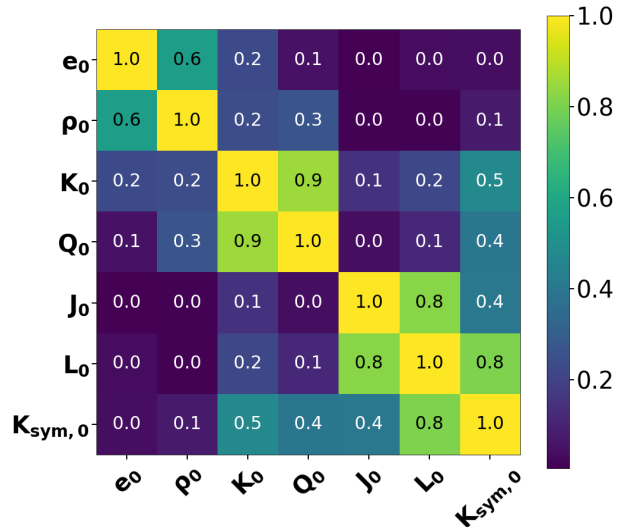


Figure 1. Correlations among various NMPs obtained using 237 selected Skyrme models from Ref. [51]. The correlations among the off-diagonal pairs  $K_0 - Q_0$ ,  $J_0 - L_0$  and  $L_0 - K_{\text{sym},0}$  are noticeable.

Before embarking on our main results, we identify the important correlations among the different NMPs using 237 Skyrme models [51, 52]. Most of these models are obtained by fitting a few selected properties of finite nuclei that impose constraints on NMPs'. In Figure 1, we present the  $7 \times 7$  matrix for the correlation coefficients obtained using Eqs. (5) and (6) for these 237 Skyrme models. The correlations among  $K_0 - Q_0, J_0 - L_0$  and  $L_0 - K_{\text{sym},0}$  pairs are noticeable. It may be emphasized that all the seven NMPs considered can be varied more or

less independently within the Skyrme model. The correlations among the NMPs are the reflections of constraints imposed by finite nuclei. The strong  $L_0 - K_{\text{sym},0}$  correlation has also been observed earlier for other nuclear models [29, 31, 53–55].

To elucidate the difference in results between the CCA and that based on the MVGD of NMPs, We generate three different distributions of the NMPs, namely, Case-I, Case-II and Case-III and obtain the corresponding sets of the Skyrme EoSs. The mean values and the errors on each of the NMPs are exactly the same for the Cases I and II as listed in Table I. The Case I corresponds to the independent distribution of NMPs, i.e., the correlation among different NMPs are ignored. In the Case II the  $L_0 - K_{\text{sym},0}$  correlation is switched on and the correlation coefficient is assumed to be 0.8. We observe that the results for the tidal deformability of neutron stars are mainly sensitive to the  $L_0 - K_{\text{sym},0}$  correlations, thus, other correlations among NMPs as seen in Fig. 1 are not considered here. The Case III is similar to Case II but the values of  $e_0$ ,  $\rho_0$ ,  $K_0$  and  $Q_0$  are kept fixed to their mean values. The distributions of NMPs for all the three Cases are filtered out such that the EoSs satisfy the causality condition and yield the maximum mass of NS above  $1.8 M_\odot$ . The central value for the maximum NS mass for each of the distributions is  $\sim 2.01 M_\odot$ . The number of filtered EoSs for each of the distributions is about 3000. These three distributions will allow us to unmask how the existing correlations among the NMPs may affect the correlation between the NS properties and the NMPs, and how much the uncertainty on the NMPs will destroy possible existing correlations. The Case III is considered in view of the small uncertainties on the isoscalar nuclear matter parameters obtained within the CCA for a Skyrme model SkA267 [38] as listed in Table I. The fit data for this model includes isoscalar and isovector giant resonances properties of finite nuclei as discussed above together with the maximum NS mass. The correlation coefficient among  $L_0 - K_{\text{sym},0}$  is 0.9 for the SkA267 model. It may be noticed from Table I that the central values for the NMPs for the different Cases considered are somewhat different from those for the SkA267 model. We will see below that the trends of the results are mainly governed by the uncertainties and the correlations among different NMPs.

In Figure 2 we plot the confidence ellipses for  $\Lambda_M$  versus  $L_0$  and  $K_{\text{sym},0}$  for NS mass  $M = 1, 1.4$  and  $1.8 M_\odot$  obtained for the Cases I, II and III and compare them with the ones for the SkA267 model obtained within the CCA. The central values for  $\Lambda_M$ ,  $L_0$  and  $K_{\text{sym},0}$  for Cases I, II and III are matched to those for the SkA267 model for the appropriate comparison. Through this comparisons, we would like to identify the reasons which can be attributed to the marked differences in the correlations of the tidal deformability with  $L_0$  and  $K_{\text{sym},0}$  as reported earlier [23, 42, 43]. The values of correlation coefficients for the results presented in the figure are summarized in Table II. Sometimes, the calculations are performed by

Table II. The values of the correlation coefficients for  $\Lambda_{1.0,1.4,1.8}$  with  $L_0$  and  $K_{\text{sym},0}$  for three different Cases considered and compared with those for SkA267.

		$\Lambda_{1.0}$	$\Lambda_{1.4}$	$\Lambda_{1.8}$
Case I	$L_0$	0.82	0.56	0.22
	$K_{\text{sym},0}$	0.26	0.58	0.71
Case II	$L_0$	0.9	0.83	0.7
	$K_{\text{sym},0}$	0.84	0.86	0.8
Case III	$L_0$	0.96	0.91	0.82
	$K_{\text{sym},0}$	0.92	0.97	0.98
SkA267	$L_0$	0.92	0.85	0.76
	$K_{\text{sym},0}$	0.89	0.94	0.98

ignoring the correlation among NMPs, which is analogous to our Case I. This yields weak correlations as seen earlier [42]. For instance, correlations of  $\Lambda_{1.0,1.4,1.8}$  with  $K_{\text{sym},0}$  are  $r \sim 0.3 - 0.7$ . The narrowing of the confidence ellipses for Case II indicate stronger correlations of  $\Lambda_{1.0}$  and  $\Lambda_{1.4}$  with  $L_0$  and  $K_{\text{sym},0}$ ,  $r \sim 0.8 - 0.9$ , while, these correlations become moderate for  $\Lambda_{1.8}$ . The SkA267 model predicts stronger correlations for  $\Lambda_M - L_0$  and  $\Lambda_M - K_{\text{sym},0}$  pairs for all NS masses considered. The  $\Lambda_M - L_0$  correlations decrease only marginally with increasing mass of NS and  $\Lambda_M - K_{\text{sym},0}$  correlations show the opposite trend. Upon examining closely we notice that the uncertainties obtained for the isoscalar NMPs such as  $e_0$ ,  $\rho_0$ ,  $K_0$  and  $Q_0$  for the SkA267 model are smaller than those employed for the Case I and II (see Table I). Thus it appears that the larger uncertainties on  $e_0$ ,  $\rho_0$ ,  $K_0$  and  $Q_0$  are also responsible for masking or reducing the correlations of  $\Lambda_{1.8}$  with  $L_0$  and  $K_{\text{sym},0}$  for the Cases I and II. These observations are reinforced in Case III by freezing the values of the isoscalar NMPs to their central values. The results for Case III are in qualitative agreement with those for SkA267. These results emphasize that the correlation of the tidal deformability with  $L_0$  and  $K_{\text{sym},0}$  are sensitive to the distributions of the NMPs used. In particular, the correlations are weaker if the NMPs are independently varied. The distribution of NMPs should be consistent with the finite nuclei data and the other relevant observables. The interplay of isoscalar NMPs such  $K_0$  and  $Q_0$  in masking the correlations of  $\Lambda_M$  with  $L_0$  and  $K_{\text{sym},0}$  can be qualitatively understood from the Taylor expansion of EoS,

$$\begin{aligned} \tilde{\epsilon}(\rho, \delta) \approx & e_0 + J_0 \delta^2 + L_0 \epsilon \delta^2 + \frac{1}{2}(K_0 + K_{\text{sym},0} \delta^2) \epsilon^2 \\ & + \frac{1}{6}(Q_0 + Q_{\text{sym},0} \delta^2) \epsilon^3 + \dots \end{aligned} \quad (7)$$

where,  $\epsilon = \frac{\rho - \rho_0}{3\rho_0}$ . It is evident from the above equation that for the pure neutron matter (i.e.  $\delta = 1$ ), the isoscalar parameters  $K_0$  is tangled with  $K_{\text{sym},0}$  so that if  $K_0$  increases,  $K_{\text{sym},0}$  decreases and vice versa; so is the case with  $Q_0$  and  $Q_{\text{sym},0}$ . For the  $\beta$ -equilibrated matter, the asymmetry  $\delta$  usually decreases with the density,

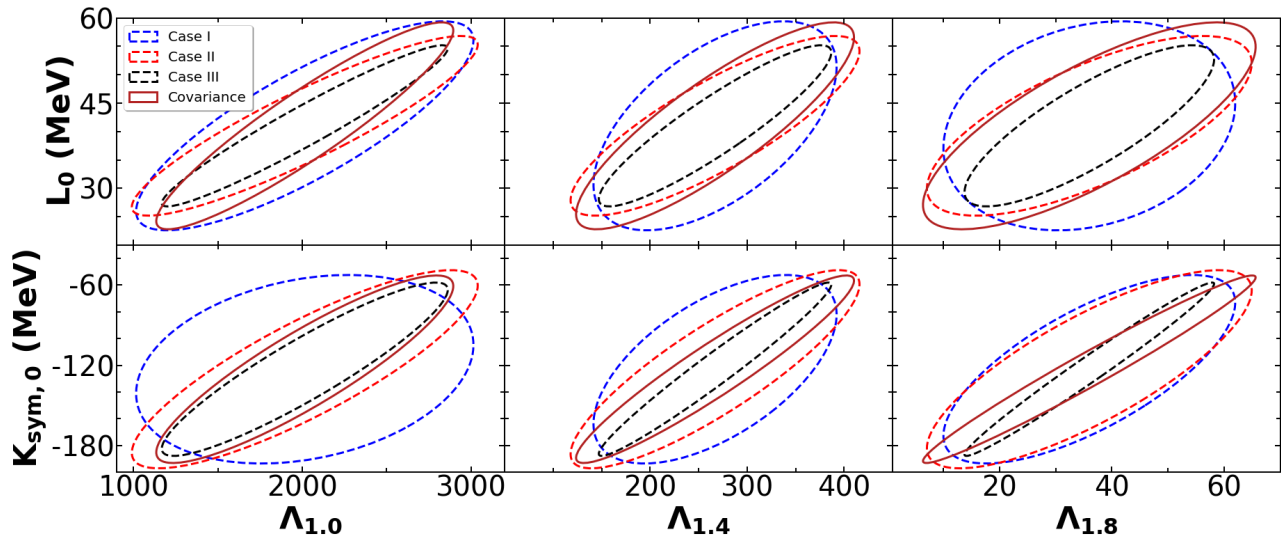


Figure 2. The  $1\sigma$  confidence ellipses in the planes of  $\Lambda_M - L_0$  (top) and  $\Lambda_M - K_{\text{sym},0}$  (bottom) with  $M = 1.0, 1.4$  and  $1.8 M_\odot$  obtained for the Case I, II and III and SkA267. The central values of all the quantities for all the Cases are matched to those for SkA267 for the appropriate comparison. The actual central values for these Cases are  $L_0 = 60$ ,  $K_{\text{sym},0} = -100$ ,  $\Lambda_{1.0} = 3200$ ,  $\Lambda_{1.4} = 430$  and  $\Lambda_{1.8} = 60$ .

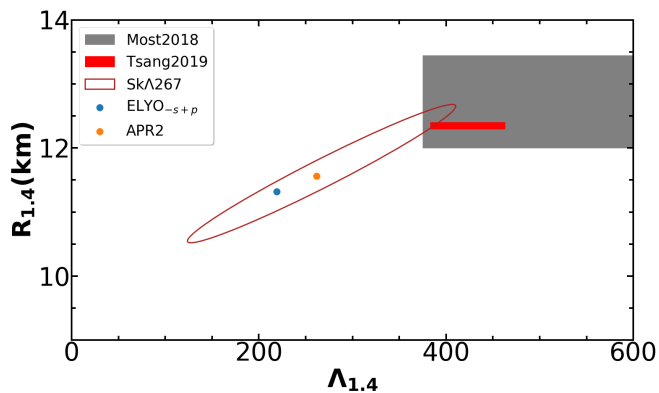


Figure 3. The  $1\sigma$  confidence ellipse in the plane of  $\Lambda_{1.4} - R_{1.4}$  for SkA267 model compared with some recent results [14, 57–59].

since, the proton fraction increases with density [56]. For the neutron stars with mass  $\sim 1M_\odot$ ,  $\epsilon < 1$ ,  $\delta \approx 1.0$  at the center, the properties of the stars are predominantly governed by  $L_0$ . On the other hand, near the maximum mass  $M_{\text{max}} \sim 2.0M_\odot$ , which corresponds to the central densities having  $\epsilon \gtrsim 1$ ,  $\delta \approx 0.4 - 0.8$ , their properties are governed by  $K_0$ ,  $Q_0$ . At the intermediate masses, both the isoscalar and isovector NMPs play an important role in determining the properties of neutron stars [33]. Since, the values of  $\epsilon_0$ ,  $\rho_0$ ,  $K_0$  and  $Q_0$  are tightly determined by our fit data, it facilitates in identifying the correlations of the  $\Lambda$  with  $L_0$  and  $K_{\text{sym},0}$ .

In Figure 3, we plot the variation of  $\Lambda_{1.4}$  with  $R_{1.4}$ . The brown ellipse is the bound obtained from SkA267 model within the  $1\sigma$  confidence. This bound has good

overlap with the recent result obtained with APR2 [59] and ELYO $_{-s+p}$  [58] and agrees marginally with the ones obtained by Most *et al.* [14] and Tsang *et al.* [57]. It may be pointed out that the results for Most *et al.* is within  $2\sigma$  limits and obtained without considering bounds from microscopic finite nuclei experiments.

*Conclusions*– The chi-square based covariance approach has been applied to evaluate the correlations of the tidal deformability  $\Lambda$  of neutron stars with the slope ( $L_0$ ) and curvature ( $K_{\text{sym},0}$ ) of the nuclear symmetry energy. This approach enables one to calculate correlation among any desired observables for a given set of fit data without a prior knowledge of the distribution of the nuclear matter parameters. The correlated distribution of NMPs in turn can be constructed in this approach in a consistent manner through the Hessian matrix which implicitly depends on the fit data. The correlations of  $\Lambda$  with  $L_0$  and  $K_{\text{sym},0}$  are also evaluated by employing explicitly a multivariate Gaussian distribution of NMPs corresponding to commonly used values for their mean and variances with and without inclusion of  $L_0 - K_{\text{sym},0}$  correlation. Comparison of the results from the multivariate Gaussian distribution with those from the chi-square based covariance approach indicates that, in order to study the correlation systematics involving tidal deformability of neutron stars, the use of multivariate distribution of the nuclear matter parameters must be appropriately guided by a realistic and as complete as possible set of fit data. Employing a set of EoS which corresponds to uncorrelated distribution of NMPs or even a correlated distribution inconsistent with fit data may mask realistic correlations that constrained nuclear models would be able to identify. The narrowing down of the difference in distributions of NMPs between Case III

where the isoscalar uncertainties are frozen and that for SkA267 where the isoscalar uncertainties are small also possibly points out to the importance of an interplay between the isoscalar and isovector NMPs. The role of the distribution of NMPs on the correlation systematics and their sensitivity to various fit data need to be further investigated within the Bayesian analysis to unveil further the information content of the tidal deformability.

*Acknowledgement*– We would like to acknowledge

Chiranjib Mondal and Bharat Kumar for the discussions and their suggestions. C.P. acknowledges financial support by Fundação para a Ciência e Tecnologia (FCT) Portugal under projects UID/FIS/04564/2019, UID/FIS/04564/2020, and POCI-01-0145-FEDER-029912. J.N.D. acknowledges support from the Department of Science and Technology, Government of India with grant no. EMR/2016/001512.

- 
- [1] P. Haensel, A. Potekhin, and D. Yakovlev, *Neutron stars 1: Equation of state and structure*, Vol. 326 (Springer, New York, USA, 2007).
- [2] J. M. Lattimer and M. Prakash, *Phys. Rept.* **621**, 127 (2016).
- [3] L. Rezzolla, P. Pizzochero, D. I. Jones, N. Rea, and I. Vidana, eds., *The Physics and Astrophysics of Neutron Stars*, Vol. 457 (Springer, 2018).
- [4] Z. Arzoumanian *et al.* (NANOGrav), *Astrophys. J. Suppl.* **235**, 37 (2018).
- [5] J. Antoniadis *et al.*, *Science* **340**, 6131 (2013).
- [6] H. T. Cromartie *et al.*, *Nature Astronomy* **4**, 72 (2019).
- [7] K. C. Gendreau *et al.*, *Proc. of SPIE* **9905**, 99051H (2016).
- [8] Z. Arzoumanian *et al.*, *Proc. of SPIE* **9144**, 914420 (2014).
- [9] A. L. Watts *et al.*, *Sci. China Phys. Mech. Astron.* **62**, 29503 (2019).
- [10] C. A. Wilson-Hodge *et al.*, *Proc. SPIE Int. Soc. Opt. Eng.* **9905**, 99054Y (2016).
- [11] C. Motch *et al.*, (2013), arXiv:1306.2334 [astro-ph.HE].
- [12] A. Bauswein, O. Just, H.-T. Janka, and N. Stergioulas, *Astrophys. J.* **850**, L34 (2017).
- [13] Y. Lim and J. W. Holt, *Phys. Rev. Lett.* **121**, 062701 (2018).
- [14] E. R. Most, L. R. Weih, L. Rezzolla, and J. Schaffner-Bielich, *Phys. Rev. Lett.* **120**, 261103 (2018).
- [15] T. Malik, N. Alam, M. Fortin, C. Providência, B. K. Agrawal, T. K. Jha, B. Kumar, and S. K. Patra, *Phys. Rev. C* **98**, 035804 (2018).
- [16] D. Radice and L. Dai, *Eur. Phys. J. A* **55**, 50 (2019).
- [17] M. Miller *et al.*, *Astrophys. J. Lett.* **887**, L24 (2019).
- [18] T. E. Riley *et al.*, *Astrophys. J. Lett.* **887**, L21 (2019).
- [19] B. P. Abbott, R. Abbott, T. D. Abbott, and F. *et al.* Acernese, *Phys. Rev. Lett.* **119**, 161101 (2017).
- [20] D. Radice, A. Perego, F. Zappa, and S. Bernuzzi, *Astrophys. J. Lett.* **852**, L29 (2018).
- [21] S. De, D. Finstad, J. M. Lattimer, D. A. Brown, E. Berger, and C. M. Biwer, *Phys. Rev. Lett.* **121**, 091102 (2018), [Erratum: *Phys. Rev. Lett.* **121**, no.25, 259902 (2018)].
- [22] E. Annala, T. Gorda, A. Kurkela, and A. Vuorinen, *Phys. Rev. Lett.* **120**, 172703 (2018).
- [23] F. J. Fattoyev, J. Piekarewicz, and C. J. Horowitz, *Phys. Rev. Lett.* **120**, 172702 (2018).
- [24] I. Tews, J. Margueron, and S. Reddy, *Phys. Rev. C* **98**, 045804 (2018).
- [25] E. E. Flanagan and T. Hinderer, *Phys. Rev. D* **77**, 021502 (2008).
- [26] T. Hinderer, *Astrophys. J.* **677**, 1216 (2008).
- [27] T. Hinderer, B. D. Lackey, R. N. Lang, and J. S. Read, *Phys. Rev. D* **81**, 123016 (2010).
- [28] T. Damour, A. Nagar, and L. Villain, *Phys. Rev. D* **85**, 123007 (2012).
- [29] I. Vidana, C. Providencia, A. Polls, and A. Rios, *Phys. Rev. C* **80**, 045806 (2009).
- [30] C. Ducoin, J. Margueron, and C. Providência, *Eur. Phys. Lett.* **91**, 32001 (2010).
- [31] C. Ducoin, J. Margueron, C. Providencia, and I. Vidana, *Phys. Rev. C* **83**, 045810 (2011).
- [32] W. Newton, M. Gearheart, and B.-A. Li, *Astrophys. J. Suppl.* **204**, 9 (2013).
- [33] N. Alam, B. Agrawal, M. Fortin, H. Pais, C. Providência, A. R. Raduta, and A. Sulaksono, *Phys. Rev. C* **94**, 052801(R) (2016).
- [34] B. K. Agrawal, T. Malik, J. N. De, and S. K. Samaddar, (2020), arXiv:2006.05758 [nucl-th].
- [35] J. N. De, S. Samaddar, and B. K. Agrawal, *Phys. Rev. C* **92**, 014304 (2015).
- [36] C. Mondal, B. K. Agrawal, J. N. De, and S. K. Samaddar, *Int. J. Mod. Phys. E* **27**, 1850078 (2018).
- [37] X. Roca-Maza, M. Centelles, X. Vinas, and M. Warda, *Phys. Rev. Lett.* **106**, 252501 (2011).
- [38] T. Malik, B. K. Agrawal, J. N. De, S. K. Samaddar, C. Providência, C. Mondal, and T. K. Jha, *Phys. Rev. C* **99**, 052801 (2019).
- [39] P. G. Krastev and B.-A. Li, *Comments Nucl. Part. Phys.* **46**, 074001 (2019).
- [40] N.-B. Zhang, B.-A. Li, and J. Xu, *Astrophys. J.* **859**, 90 (2018).
- [41] N.-B. Zhang and B.-A. Li, *Eur. Phys. J. A* **55**, 39 (2019).
- [42] Z. Carson, A. W. Steiner, and K. Yagi, *Phys. Rev. D* **99**, 043010 (2019).
- [43] M. Ferreira, M. Fortin, T. Malik, B. Agrawal, and C. Providência, *Phys. Rev. D* **101**, 043021 (2020).
- [44] H. Güven, K. Bozkurt, E. Khan, and J. Margueron, (2020), arXiv:2001.10259 [nucl-th].
- [45] J. Margueron, R. Hoffmann Casali, and F. Gulminelli, *Phys. Rev. C* **97**, 025805 (2018).
- [46] J. Margueron, R. Hoffmann Casali, and F. Gulminelli, *Phys. Rev. C* **97**, 025806 (2018).
- [47] P.-G. Reinhard and W. Nazarewicz, *Phys. Rev. C* **81**, 051303 (2010).
- [48] J. Dobaczewski, W. Nazarewicz, and P.-G. Reinhard, *J. Phys. G* **41**, 074001 (2014).
- [49] C. Mondal, B. K. Agrawal, and J. N. De, *Phys. Rev. C* **92**, 024302 (2015).
- [50] S. Brandt, *Statistical and Computational Methods in Data Analysis* (Springer, New York, 3rd English edition, 1997).

- [51] M. Dutra, O. Lourenco, J. S. Sa Martins, A. Delfino, J. R. Stone, and P. D. Stevenson, *Phys. Rev.* **C85**, 035201 (2012).
- [52] C. Mondal, B. K. Agrawal, J. N. De, S. K. Samaddar, M. Centelles, and X. Viñas, *Phys. Rev.* **C96**, 021302 (2017).
- [53] L.-W. Chen, B.-J. Cai, C. M. Ko, B.-A. Li, C. Shen, and J. Xu, *Phys. Rev. C* **80**, 014322 (2009).
- [54] P. Danielewicz and J. Lee, *Nucl. Phys. A* **818**, 36 (2009).
- [55] C. Providência, S. S. Avancini, R. Cavagnoli, S. Chiacchiera, C. Ducoin, F. Grill, J. Margueron, D. P. Menezes, A. Rabhi, and I. Vidaña, *Eur. Phys. J. A* **50**, 44 (2014).
- [56] G. Fiorella Burgio and A. F. Fantina, in *The Physics and Astrophysics of Neutron Stars*, edited by L. Rezzolla, P. Pizzochero, D. I. Jones, N. Rea, and I. Vidaña (Springer Int. Pub, Cham, 2018) pp. 255–335.
- [57] C. Tsang, B. Brown, F. Fattoyev, W. Lynch, and M. Tsang, *Phys. Rev. C* **100**, 062801 (2019).
- [58] J. Bonnard, M. Grasso, and D. Lacroix, *Phys. Rev. C* **101**, 064319 (2020).
- [59] A. Sabatucci and O. Benhar, (2020), arXiv:2001.06294 [nucl-th].